

Quantitative analysis of dynamic-force-spectroscopy data on graphite(0001) in the contact and noncontact regimes

H. Hölscher,* A. Schwarz, W. Allers, U. D. Schwarz, and R. Wiesendanger

Institute of Applied Physics and Microstructure Research Center, University of Hamburg, Jungiusstrasse 11, D-20355 Hamburg, Germany

(Received 19 January 2000)

We present a comparative experimental and theoretical study of the frequency shift in ultrahigh vacuum dynamic force microscopy at 80 K on graphite(0001) measured as a function of the tip-sample distance for different resonance amplitudes A in the repulsive and attractive regime of the tip-sample forces. The resulting frequency shift versus distance curves scale with $1/A^{3/2}$ over the full range. We determined the tip-sample force from the frequency shift versus distance curves and found good agreement with specific force laws for long-range (van der Waals), short-range (Lennard-Jones), and contact (Hertz) forces.

With the successful application of the so-called *dynamic* or *noncontact* mode¹ of the *atomic force microscope*² (AFM) using large amplitudes, it became possible to achieve “true” atomic resolution, e.g., on Si(111)7×7,^{3,4} which is comparable to the resolution obtained by *scanning tunneling microscopy*.⁵ Despite this experimental success, the origin of the contrast mechanism is still under discussion. For example, it was suggested that strong interactions through dangling bonds between the foremost tip atoms and the surface atoms are responsible for the observed contrast.^{4,6} However, it is also possible to obtain atomic-scale contrast on *van der Waals* surfaces like graphite(0001) (Ref. 7) and xenon(111) (Ref. 8). Another important question is whether the high resolution is really obtained in a true noncontact mode.⁹ Consequently, it is of high interest to examine the tip-sample interactions occurring in dynamic force microscopy in more detail.

In order to get insight into the tip-sample interaction, we measured the frequency shift Δf in dependence of the tip-sample distance for different resonance amplitudes A . Since it was the aim of this study to measure the tip-sample interaction in the *noncontact* and in the *contact* regime, we chose (0001)-oriented graphite as a sample. It is well known that this material consists of individual layers of hexagonally arranged carbon atoms; within these layers each atom is strongly bound by sp^2 bonds. Therefore, we expect no damage of the sample surface, if the tip touches the sample only slightly. Analyzing the measured frequency shift versus distance curves, we found that the frequency shift scales with $1/A^{3/2}$ as predicted earlier.¹⁰ To fit the experimental data to specific force laws (van der Waals, Lennard-Jones, Hertz, we calculated the tip-sample interaction force from the frequency shift curves. The subsequent analysis demonstrates that *dynamic force spectroscopy* can be used to measure tip-sample interactions including elastic contact forces with high precision.

The experiments were carried out with a home-built atomic force microscope designed for operation in ultrahigh vacuum (UHV) and at low temperatures. The AFM, which has already been described in detail elsewhere,¹¹ works with an all-fiber interferometer and is cooled in a bath cryostat.

Sample and cantilever are prepared and mounted in UHV. The rectangular-shaped cantilever used for this study was made of monocrystalline silicon with a spring constant of 38 N/m and an eigenfrequency of 171 kHz. The tip was sputtered *in situ* with Ar^+ ions prior to the measurements. The graphite sample was cleaved *in situ* at room temperature at a pressure below 10^{-9} mbar and immediately inserted into the precooled microscope (base pressure below 10^{-10} mbar). After the sample reached an equilibrium temperature at $T = 80$ K (liquid-nitrogen cooling), a series of experiments were performed measuring the frequency shift Δf as a function of the tip-sample distance for different resonance amplitudes A . The experimental data presented here were recorded with grounded tip and sample.

The obtained frequency shift versus distance curves are presented in Fig. 1(a) by symbols for resonance amplitudes between 54 and 180 Å. All curves show a similar overall shape. During the approach of the cantilever to the sample surface, the frequency shift decreases and reaches a minimum. With a further reduction of the nearest tip-sample distance, the frequency shift increases again and becomes positive. For smaller resonance amplitudes, the minimum of the $\Delta f(z)$ curves is deeper and the slope after the minimum is steeper than for larger amplitudes.

The frequency shift versus distance curves can be rescaled to a *normalized frequency shift curve*¹⁰

$$\gamma(z) := \frac{c_z A^{3/2}}{f_0} \Delta f(z), \quad (1)$$

which should be independent of the spring constant c_z , the eigenfrequency f_0 , and the amplitude A of the cantilever. The dependence of the frequency shift on these parameters has first been calculated for the specific case of inverse power and exponential force laws,¹⁰ but the same result can be obtained for arbitrary tip-sample forces.¹² The application of this scaling law to our experimental data is plotted in Fig. 1(b). All data points perfectly fit to a single curve within the full range, demonstrating the validity of the predicted $1/A^{3/2}$ dependence of the frequency shift. This result verifies that γ is a useful quantity to compare frequency shift versus distance curves acquired with different amplitudes.

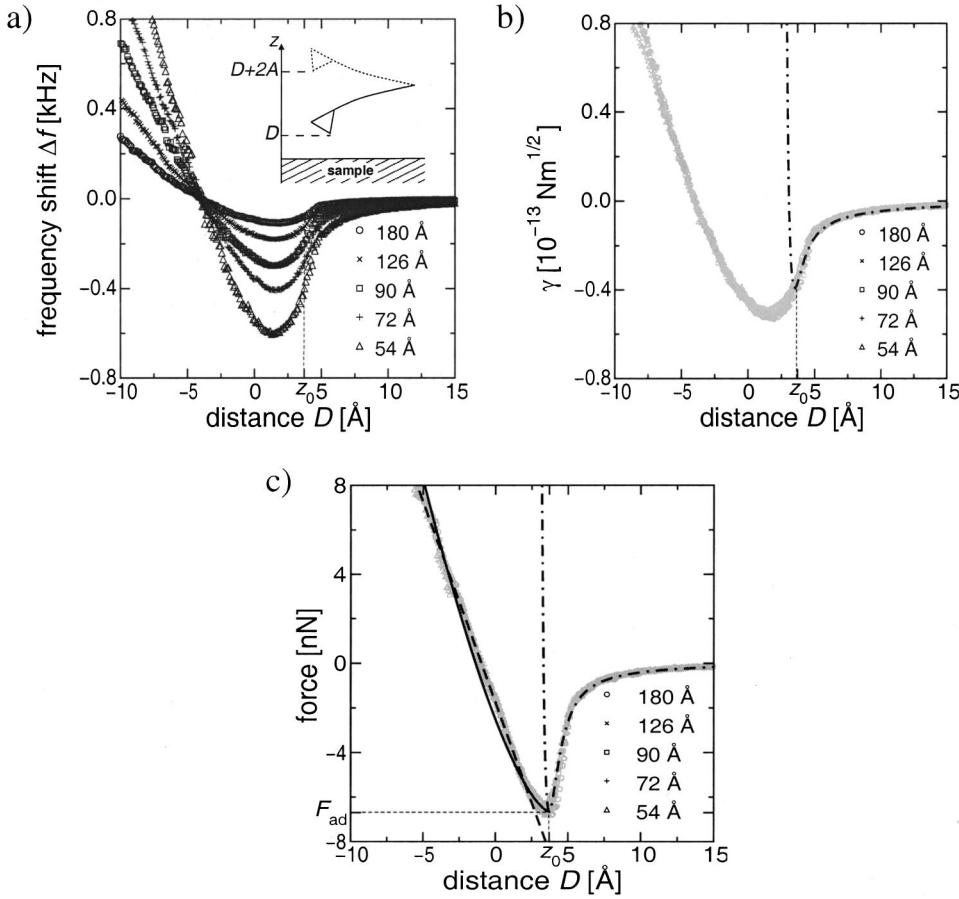


FIG. 1. (a) The experimental frequency shift versus distance curves acquired with a silicon tip and a graphite sample for different amplitudes are displayed by symbols. All curves are shifted along the x axes. The zero point is defined by the force law Eq. (2). Inset: definition of the parameters A and D . (b) The normalized frequency shift γ as a function of D obtained from the experimental data presented in (a). The dashed-dotted line represents the best fit using Eq. (3). (c) The tip-sample force calculated with the experimental data given in (a) using Eq. (4) is shown by symbols. The force F_{ts} Eq. (2) is plotted by a dashed-dotted line. The best fit using the force law F_c is displayed by a solid line; a linear fit for $D < 0$ Å is drawn by a dashed line. To indicate the border between ‘‘contact’’ and ‘‘noncontact’’ force, the position z_0 is marked in all plots.

However, to obtain more information on the tip-sample interaction from the $\Delta f(z)$ curves, it is useful to calculate the frequency shift for suitable tip-sample interaction forces and to compare these results with the experiment. Giessibl¹⁰ suggested to describe the force between the tip and the sample by a combination of a long-range (van der Waals) and a short-range (Lennard-Jones) terms. For a tip with the radius R , this assumption results in the tip-sample force

$$F_{ts}(z) = -\frac{A_H R}{6z^2} + \frac{12E_0}{r_0} \left[\left(\frac{r_0}{z} \right)^{13} - \left(\frac{r_0}{z} \right)^7 \right], \quad (2)$$

where A_H is the Hamaker constant, E_0 the binding energy, and r_0 the equilibrium distance of the Lennard-Jones potential. Since this approach does not explicitly consider elastic contact forces, it is only valid as long as the tip and sample are not in contact. Therefore, we will call the force law Eq. (2) ‘‘noncontact’’ force in the following to distinguish it from the other force law used below to explicitly describe elastic tip-sample forces. With the formulas given in Ref. 10, the normalized frequency shift for this specific tip-sample force can be calculated in the limit of large amplitudes from

$$\gamma_{ts}(D) = -\frac{A_H R}{12\sqrt{2}D^{1.5}} + \frac{12E_0}{\sqrt{2}r_0} \left[0.16 \left(\frac{r_0}{D} \right)^{12.5} - 0.23 \left(\frac{r_0}{D} \right)^{6.5} \right], \quad (3)$$

where D is the nearest tip-sample distance during the oscillations of the cantilever [see the inset in Fig. 1(a)].

A fit of this equation to the experimentally obtained normalized frequency shift is plotted in Fig. 1(b) by a solid line;

the parameters are $A_H R = 2.4 \times 10^{-27}$ Jm, $r_0 = 3.4$ Å, and $E_0 = 3$ eV. The regime right from the minimum of the calculated curve fits well to the experimental data, but the deep and wide minimum of the experimental curves cannot be described accurately with the noncontact force Eq. (2). This is caused by the steep increase of the Lennard-Jones force in the repulsive regime ($F_{ts} \propto 1/r^{12}$ for $z < r_0$). The specific choice of the short-range force does not matter; the obtained agreement is not significantly better with other choices (e.g., a Morse potential).

To analyze the frequency shift curves behind the minimum of F_{ts} , it is useful to change our approach to data analysis. So far, we assumed a certain tip-sample force, calculated the frequency shift caused by this force, and compared the result with the experimental data. An alternative and probably more instructive way is to directly calculate the interaction force from the frequency shift, which can be done either by the analysis of the frequency shift as a function of the distance^{12,13} or of the amplitude.¹⁴ Here, we determine the tip-sample force using the approach of Dürig¹² leading to the formula

$$F_{int}(D) = \sqrt{2} \frac{c_z A^{3/2}}{f_0} \frac{\partial}{\partial D} \int_D^\infty \frac{\Delta f(z)}{\sqrt{z-D}} dz, \quad (4)$$

which allows the calculation of the tip-sample interaction force from the frequency shift versus distance curves.

The application of this method results in identical tip-sample force curves for the different resonance amplitudes, as shown in Fig. 1(c). This demonstrates that the tip-sample

interaction did not change during the measurement, i.e., inelastic deformations of the sample and/or tip changes during the recording of the presented data can be excluded. The comparison with the force law F_{ts} Eq. (2) (dashed-dotted line) confirms our former result that this force law fits the tip-sample interaction force quite well, but only to the ‘right’ of the minimum of F_{ts} . If the tip comes closer to the sample surface, the repulsive forces between tip and sample become more pronounced. Consequently, tip and sample are deformed by elastic contact forces, which we will discuss in the following.

To obtain a contact force law, we assume that the form of tip and sample changes only slightly until point contact is reached and that, after the formation of this point contact, the tip-sample forces are given by the Hertz theory.^{15,16} This approach coincides with the model of Derjaguin, Muller, and Toporov (DMT)¹⁷ and has been successfully used to describe the tip-sample contact of an AFM.^{18,19} It results in a force law of the type

$$F_c = g_0(z_0 - z)^{3/2} + F_{ad} \quad \text{for } z \leq z_0. \quad (5)$$

The first term in this equation describes the elastic behavior of a Hertzian contact, where z_0 is the point of contact, and g_0 is a constant that depends on the elasticity of tip and sample, and on the shape of the tip.²⁰ The offset F_{ad} is the adhesion force between tip and sample surface. Since the experimental tip-sample force shows a reasonable agreement with the non-contact force [Eq. (2)] until its minimum, we defined the contact point by this minimum, i.e., $z_0 := \min\{F_{ts}(z)\} = 3.7 \text{ \AA}$ and therefore, $F_{ad} := F_{ts}(z_0) = -6.7 \text{ nN}$. With this choice, we get not only a continuous connection between the noncontact and contact force, but also between their force gradients.

A fit of Eq. (5) to the experimental data is shown in Fig. 1(c) by a solid line ($g_0 = 5.8 \times 10^5 \text{ nN/m}^{3/2}$). The good agreement with the experimental force curves demonstrates that the contact force describes the tip-sample interaction much better than the repulsive part of the noncontact force F_{ts} since contact forces obviously dominate the tip-sample interaction for $D < z_0$. It is additionally interesting to note that the described analysis allows us to identify the border between the noncontact and contact regime in the frequency shift versus amplitude curves. As shown in Fig. 1(a), the

contact point z_0 is near the point of inflection of the $\Delta f(z)$ curves, well before the minimum of the $\Delta f(z)$ curves.

Although the DMT model gives reasonable agreement with the overall behavior of the measured data for $D < z_0$, it should be mentioned that the experimental force curve looks quite linear for $D < 0 \text{ \AA}$. Fitting a linear force law to the measured data within this range [see the dashed line in Fig. 1(c)] leads to a contact stiffness of $\approx 18 \text{ N/m}$. A similar behavior has been reported for the single asperity contact investigated in Ref. 21, whereas other authors^{18,19} found a better agreement with the Hertz/DMT force law as already mentioned above. The main reason for these different results might be the specific choice of the tip/sample materials used in each case. However, another possible reason is that the consideration of the attractive adhesion forces by a constant offset is incomplete. Consequently, in order to examine the validity of specific force laws describing the contact mechanics of a single asperity contact, it will be the aim of future research to use well-defined (e.g., spherical²²) tips on different samples, and to compare the experimental results with models considering the adhesion forces in a more sophisticated way, see, e.g., Refs. 23–25.

In summary, we presented a comparative experimental and theoretical study of the frequency shift in dynamic force microscopy on graphite (0001) in dependence of the tip-sample distance and the resonance amplitude. It was verified that frequency shift versus distance curves obtained with different amplitudes scale with $1/A^{3/2}$ and can therefore be condensed to a single normalized frequency shift curve. To fit the experimental data to specific force laws, we determined the tip-sample force from the frequency shift versus distance curves. This experimental force curve shows good agreement with specific force laws for long-range (van der Waals), short-range (Lennard-Jones), and contact (Hertz/DMT) forces. The result demonstrates that not only noncontact, but also elastic contact forces can be quantitatively measured by dynamic force spectroscopy opening a new and direct way to the verification of contact mechanical models of nanoasperities.

Financial support from the Deutsche Forschungsgemeinschaft (Grant No. WI1277/2-3), the BMBF (Grant No. 13N6921/3), and the Graduiertenkolleg ‘‘Physik Nanostrukturierter Festkorper’’ is gratefully acknowledged.

*Electronic address: hoelscher@physnet.uni-hamburg.de

¹T. R. Albrecht, P. Grutter, D. Horne, and D. Rugar, *J. Appl. Phys.* **69**, 668 (1991).

²G. Binnig, C. F. Quate, and Ch. Gerber, *Phys. Rev. Lett.* **56**, 930 (1986).

³F.-J. Giessibl, *Science* **267**, 68 (1995).

⁴R. Erlandsson, L. Olsson, and P. Martenson, *Phys. Rev. B* **54**, R8309 (1996).

⁵G. Binnig, H. Rohrer, Ch. Gerber, and E. Weibel, *Phys. Rev. Lett.* **50**, 120 (1983).

⁶R. Perez, M. C. Payne, I. Stich, and K. Terakura, *Phys. Rev. Lett.* **78**, 668 (1997).

⁷W. Allers, A. Schwarz, U. D. Schwarz, and R. Wiesendanger, *Appl. Surf. Sci.* **140**, 247 (1999).

⁸W. Allers, A. Schwarz, U. D. Schwarz, and R. Wiesendanger, *Europhys. Lett.* **49**, 276 (1999).

⁹I. Yu. Sokolov, G. S. Henderson, and F. J. Wicks, *Surf. Sci.* **381**, L558 (1997).

¹⁰F.-J. Giessibl, *Phys. Rev. B* **56**, 16 010 (1997).

¹¹W. Allers, A. Schwarz, U. D. Schwarz, and R. Wiesendanger, *Rev. Sci. Instrum.* **69**, 221 (1998).

¹²U. Durig, *Appl. Phys. Lett.* **75**, 433 (1999).

¹³B. Gotsmann, B. Anczykowski, C. Seidel, and H. Fuchs, *Appl. Surf. Sci.* **140**, 314 (1999).

¹⁴H. Holscher, W. Allers, U. D. Schwarz, A. Schwarz, and R. Wiesendanger, *Phys. Rev. Lett.* **83**, 4780 (1999).

¹⁵H. Hertz, and J. Reine, *Angew. Math.* **92**, 156 (1882).

¹⁶L. Landau and E. M. Lifschitz, *Lehrbuch der Theoretischen Physik IV*, 7th ed. (Akademie Verlag, Berlin, 1991).

¹⁷B. V. Derjaguin, V. M. Muller, and Yu. P. Toporov, *J. Colloid Interface Sci.* **53**, 314 (1975).

¹⁸U. D. Schwarz, O. Zworner, P. Koster, and R. Wiesendanger, *Phys. Rev. B* **56**, 6987 (1997).

- ¹⁹ Enachescu, R. J. A. van den Oetelaar, R. W. Carpick, D. F. Ogletree, C. F. J. Flipse, and M. Salmeron, Phys. Rev. Lett. **81**, 1877 (1998).
- ²⁰ If the tip is exactly spherical with the radius R , the constant g_0 is given by $g_0 = K\sqrt{R}$, where $K = \frac{4}{3}[(1 - \nu_1^2)/E_1 + (1 - \nu_2^2)/E_2]^{-1}$ describes the elasticity of tip and sample ($E_{1,2}$ is Young's moduli, $\nu_{1,2}$ is the Poisson ratio of tip and sample, respectively). If the exact geometry of the tip is unknown, the constant g_0 cannot be determined *a priori*, but it can be shown that Eq. (5) still holds (Ref. 16).
- ²¹ G. Cross, A. Schirmeisen, A. Stadler, P. Grütter, M. Tschudy, and U. Dürig, Phys. Rev. Lett. **80**, 4685 (1998).
- ²² U. D. Schwarz, O. Zwörner, P. Köster, and R. Wiesendanger, J. Vac. Sci. Technol. B **15**, 1527 (1997).
- ²³ V. M. Muller, V. S. Yushchenko, and B. V. Derjaguin, J. Colloid Interface Sci. **77**, 91 (1980).
- ²⁴ V. M. Muller, V. S. Yushchenko, and B. V. Derjaguin, J. Colloid Interface Sci. **92**, 92 (1982).
- ²⁵ D. Maugis, J. Colloid Interface Sci. **150**, 243 (1991).